Research Article Vol. 2, No. 3 / 15 March 2019 / OSA Continuum 715

Gd^{3+}-doped sol-gel silica glass for remote ionizing radiation dosimetry

HICHAM EL HAMZAOUI,[1,*] GÉRAUD BOUWMANS,[1] BRUNO CAPOEN,[1] ANDY CASSEZ,[1] RÉMI HABERT,[1] YOUCEF OUERDANE,[2] SYLVAIN GIRARD,[2] DIEGO DI FRANCESCA,[3] NOURDINE KERBOUB,[3] ADRIANA MORANA,[2] DANIEL SÖDERSTRÖM,[4] AZIZ BOUKENTER,[2] AND MOHAMED BOUAZAOUI[1]

[1] *Univ-Lille, CNRS, UMR 8523 - PhLAM - Physique des Lasers Atomes et Molécules, F-59000 Lille, France*
[2] *Univ Lyon, Laboratoire H. Curien, UJM-CNRS-IOGS, 18 rue du Pr. Benoît Lauras 42000, Saint-Etienne, France*
[3] *CERN, CH-1211 Geneva, Switzerland*
[4] *Department of Physics, FI-40014 University of Jyväskylä, Finland*
[*] *hicham.elhamzaoui@univ-lille1.fr*

Abstract: Gadolinium-doped silica glass was prepared, using the sol-gel route, for ionizing radiation dosimetry applications. Such a glassy rod was drawn to a cane at a temperature of 2000 °C. The structural and optical properties of the obtained material were studied using Raman, optical absorption, and photoluminescence spectroscopies. Thereafter, a small piece of this Gd-doped scintillating cane was spliced to a transport passive optical fiber, allowing the remote monitoring of the X-ray dose rate through a radioluminescence (RL) signal. The sample exhibited a linear RL intensity response versus the dose rate from 125 μGy(SiO_2)/s up to 12.25 Gy/s. These results confirm the potentialities of this material for real-time remote ionizing radiation dosimetry.

1. Introduction

There is a great interest in elaborating and designing new material with optical activity in the UV domain. Indeed, UV-light sources are crucial for a broad range of applications in several domains, such as spectroscopy [1], medicine [2], food processing [3] and lithography [4]. Moreover, in harsh environments, dosimeters are required to monitor the radiation constraints. Such dosimeters should ideally present the remote measurement ability, in real-time and/or with a high spatial resolution. This concerns the field of new techniques for radiotherapy, as well as in space and nuclear domains [5–9]. For these applications, fibered solutions seem particularly adapted and new sensitive materials, such as rare-earth (RE) doped glasses, can be drawn into fibers. In fact, due to the optical activity in the UV domain, the incorporation of Gd^{3+} ions inside oxide glasses leads to efficient scintillator and phosphor materials [10,11]. However, in most of the investigated glasses, the Gd^{3+} ions have mainly been used as sensitizers for other rare-earth ions to enhance their luminescence [12–16]. This mostly concerned multicomponent glasses, which contain glass modifier elements, such as aluminum, that could decrease the glass resistance to radiations [17]. Pure silica glass is obviously a promising host due to its high damage threshold, physical stability and strong chemical resistance [18–22]. However, only a few studies have been devoted to Gd^{3+}-doped silica glasses without other co-dopant [23,24]. In this paper, we investigate the structural and optical properties of a Gd^{3+}-doped silica glass prepared using the sol-gel process in combination with a post-doping technique. The RL response of this active material, included as a component of a fiber-based device for X-ray radiation remote monitoring, has been evaluated over several dose rate decades for the first time to our best knowledge. It

#354970 https://doi.org/10.1364/OSAC.2.000715
Journal © 2019 Received 10 Dec 2018; revised 14 Feb 2019; accepted 15 Feb 2019; published 11 Mar 2019

OSA CONTINUUM

constitutes our preliminary results of an effort undertaken to evaluate the potential of Gd^{3+}-doped silica glasses as scintillating materials for ionizing radiation dosimetry.

2. Experiments, results, and discussion

Porous silica xerogel was prepared using the sol-gel technique from tetraethylorthosilicate (TEOS) precursor as described elsewhere [25]. The obtained xerogel was stabilized at 1000°C and then soaked in an alcoholic solution containing gadolinium salt. Subsequently, the sample was withdrawn from the doping solution and dried at 50°C for 24 hours to remove solvents and retain gadolinium element within the nanopores. The doped matrix was then densified in helium atmosphere at 1350°C for 2 hours. Finally, the Gd-doped glassy rod was drawn at a temperature of about 2000°C down to a millimeter-sized cane. The Gd concentration in the cane sample was estimated at about 0.1 wt% by electron probe micro-analysis.

Raman spectroscopy analysis was performed in a cane sample, at room temperature, in a confocal configuration using a triple-grating spectrometer (Jobin-Yvon T64000) and the 514.5 nm line of an Ar^+ laser as the excitation source.

Figure 1 presents the Raman spectrum of the Gd^{3+}-doped cane sample, which exhibits the well-known SiO_2 glass bands [26], including the large band centered around 440 cm^{-1} and attributed to the Si-O-Si network deformation vibration (ω_1). The two smaller bands at 490 cm^{-1} (D_1) and 603 cm^{-1} (D_2) are assigned to symmetric stretching modes of three- and four-member siloxane rings, respectively, in the silica network. The asymmetric band situated around 800 cm^{-1} (ω_3) is assigned to a complex vibration involving substantial silicon motion in addition to a bending movement of oxygen in a vitreous network. The high frequency bands (ω_4) at ~1050 and ~1200 cm^{-1} were attributed to a TO-LO pair splitting. Finally, in the low-frequency region, the clear band around 60 cm^{-1}, called the "Boson peak", is characteristic of the vitreous state [27].

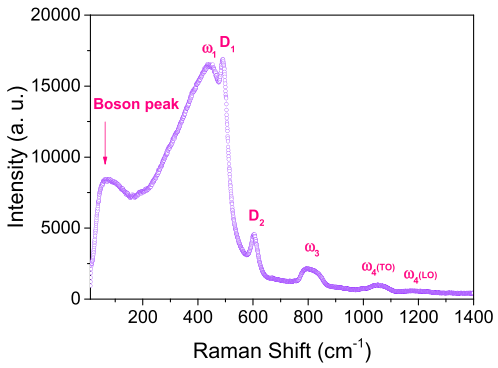

Fig. 1. Raman spectrum of Gd^{3+}-doped silica cane.

UV absorption spectrometry was performed at room temperature using a Cary 5000 double-beam spectrometer (Agilent Technologies).

The optical absorption spectrum of Gd^{3+}-doped silica cane is presented in Fig. 2. This spectrum shows two absorption band groups in the wavelength ranges from 243–258 nm and 270–280 nm. They are attributed to the transitions from the ground state ($^8S_{7/2}$) to the ^6D_J and ^6I_J excited multiplets of Gd^{3+} ions, respectively [28].

Photoluminescence (PL) kinetic measurements were performed, at room temperature, using an optical parametric oscillator equipped with a second harmonic generation nonlinear crystal pumped by the third harmonic of a Nd:YAG laser with a 5 ns pulse width and a 10 Hz repetition rate. The light emitted by the samples was spectrally resolved by a grating with 300 grooves/mm and recorded by a gated intensified CCD equipped with a delay generator. Figure 3(a) shows the

OSA CONTINUUM

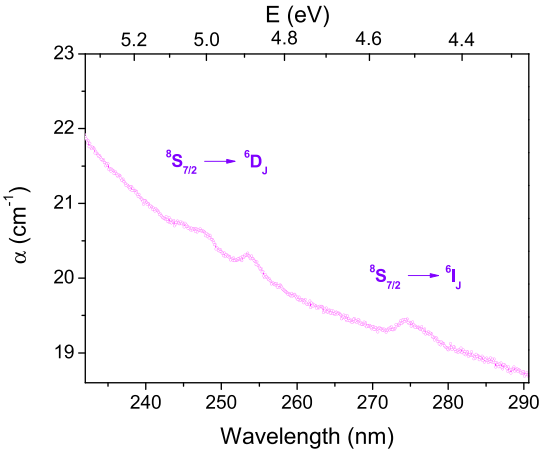

Fig. 2. Optical absorption spectrum of Gd^{3+}-doped silica cane.

PL spectrum of the glassy cane under pulsed excitation at 275 nm. As seen under this excitation, the sample presents a sharp UV PL band centered around 314 nm (3.95 eV), with a full width at half maximum (FWHM) estimated at about 3.3 nm (0.041 eV). This band corresponds to the Gd^{3+} transition between $^6P_{7/2}$ and $^8S_{7/2}$ states [29]. Figure 3(b) shows the PL decay curve recorded at 314 nm under the same excitation wavelength (275 nm) and with a time resolution of 20 μs.

We have found that this PL decay curve does not follow a pure mono-exponential function. However, it could be successfully fitted by a stretched exponential function that takes into account the multisite environment of the Gd^{3+} ions [30,31]:

$$I(t) = y_0 + A \exp\left[-\left(\frac{t}{\tau}\right)^{\beta}\right] \tag{1}$$

where I(t) is the luminescence intensity, t is time, y_0 is the background (noise level), A is the intensity at $t = 0$, β is the stretch factor and τ is a characteristic relaxation time. The fit to the above function is shown in Fig. 3(b) for the emission wavelength 314 nm, yielding the parameters $\beta = (0.86 \pm 0.01)$ and $\tau = (1.35 \pm 0.01$ ms). This result leads to the commonly used interpretation of an observed stretched exponential relaxation in glasses, which refers to the global relaxation of a system containing a number of independently relaxing species, each of which

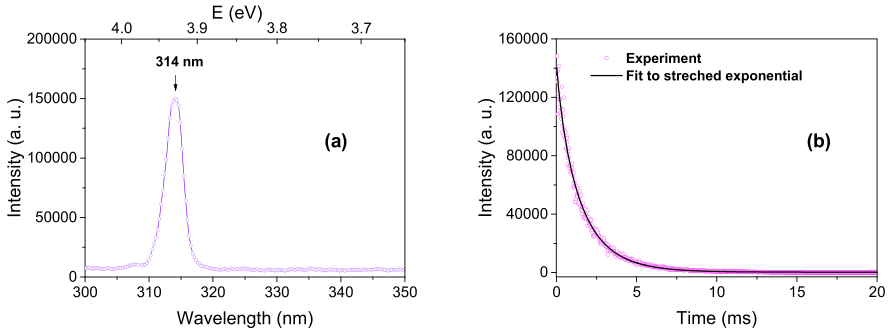

Fig. 3. (a) PL spectrum of Gd^{3+}-doped silica cane under pulsed excitation at 275 nm, (b) PL decay curve recorded at 314 nm wavelength, under excitation at 275 nm and its corresponding curve fitting using Eq. (1).

OSA CONTINUUM

decays exponentially with a specific fixed relaxation rate τ [32]. The stretched exponential nature of the PL dynamic obtained at 314 nm can be explained by a favorable role of our post-doping route using nanoporous silica xerogel, which facilitates the dispersion of gadolinium ions in the glass, reduces their ability for cluster formation and leads to disordered local environments with a multiplicity of sites available for the trivalent gadolinium ions. The obtained value of τ is close to the dominant decay time of 1.8 ms reported in the literature [23]. This former was determined from two-exponential approximation and reported in the case of Gd^{3+} ions in silica glass, with comparable doping level (0.05 mol.%), subjected to rapid thermal treatment at high temperature.

For RL measurements, the experimental setup was composed of a 0.5 mm-diameter $\times$ 10 mm-length piece of the Gd^{3+}-doped cylindrical cane, one end of which was fusion-spliced to a 5 m-long multimode silica fiber (Fig. 4). This fiber, with a core diameter of 0.5 mm coated with a low refractive index polymer clad, was used to guide the RL signal toward a photomultiplier module (PMT, H9305-03 Hamamatsu). The PMT module was connected to a numerical oscilloscope for data acquisition (Agilent Technologies InfiniiVision DSO7052B). The electrical voltage signal provided by the PMT is read by a numerical oscilloscope. The external X-ray beam was delivered by the MOPERIX facility of Laboratoire Hubert Curien, operating at 100 kV and generating photons of $\sim$ 40 keV average energy. The X-ray dose rate is driven by the electric current of the equipment and values up to 12.25 $Gy(SiO_2)$ can be reached. The transport optical fiber was not subjected to X-rays. To shield this fiber during the irradiation, we used plates of aluminum and lead. The dose rate is evaluated with an ionization chamber, calibrated to provide the dose rates in $Gy(H_2O)$/s. These values have been converted in $Gy(SiO_2)$ taking into account the ratio of mass attenuation coefficients between water and silica [33].

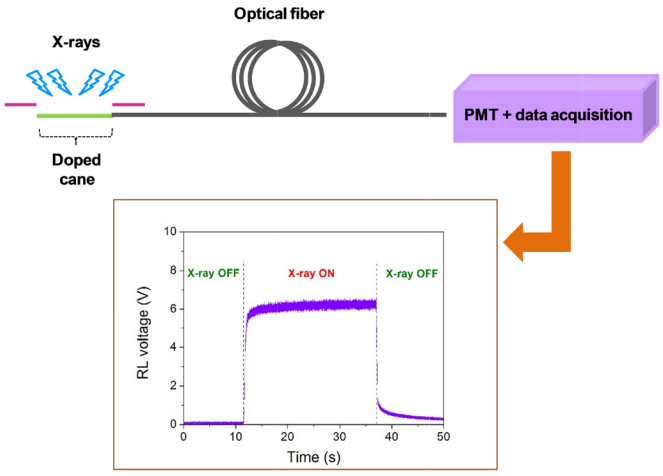

Fig. 4. Schematic illustration of the experimental setup used to characterize the RL response of Gd^{3+}-doped cane exposed to X-rays. In the bottom, RL signal evolution versus time under 427 $mGy(SiO_2)$/s.

In the bottom of Fig. 4 is shown the RL signal evolution versus time obtained at 427 $mGy(SiO_2)$/s dose rate. As the X irradiation starts, the RL signal increases and tends toward a plateau if the dose rate is constant during the run. The amplitude of this plateau depends on the dose rate level. The delayed response of the material to irradiation is attributed to carrier trap states. Indeed, during the irradiation, the prompt recombination causing the production of the RL signal is in competition with electron trapping. However, while the electron traps, including shallow and deep ones, are filled, the trapping probability decreases and then, more electrons become available for recombination. The RL signal rises to a steady-state level, which

OSA CONTINUUM

increases for each increasing dose rate [34]. After shutting down the X-ray irradiation, the signal decreases within a few seconds, then presents an afterglow behavior. This obtained response could be related to the influence of shallow traps on the process of RL [35].

Figure 5 shows the evolution of the average RL signal, in the permanent regime (plateau), as a function of the X-ray dose rate. The dose rate dependence of the RL is clearly linear from 125 μGy(SiO_2)/s to at least 12.25 Gy(SiO_2)/s. To the best of our knowledge, it is the first time such a linear response, ranging over about five decades, has been reported with a Gd^{3+}-doped silica glass.

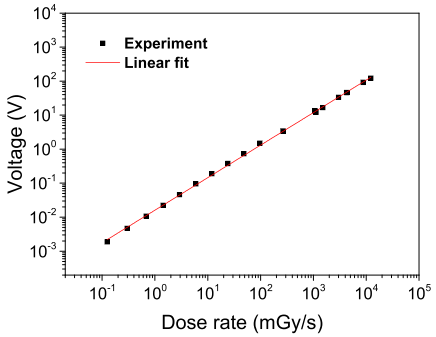

Fig. 5. RL response of the Gd^{3+}-doped cane spliced to a fiber as a function of the X-ray dose rate. The uncertainties on both dose rate and RL voltage values are estimated to be within 10% and 5%, respectively.

We performed a spectroscopic investigation to elucidate the mechanisms at the origin of the RL signal. The RL spectrum was recorded by connecting the fiber to a TM-UV/VIS mini-spectrometer (C10082CA Hamamatsu).

Figure 6(a) presents the RL spectrum of Gd^{3+}-doped cane in the whole UV-visible range obtained under 2.1 Gy(SiO_2)/s X-ray dose rate. It shows narrow and intense RL emission band centered at 314.4 nm (3.94 eV), with a FWHM of about 4.1 nm (0.051 eV). No other RL emission, related to defect centers [36], at lower energy could be detected. Moreover, no continuous background signal due to the stem effects has been observed [5]. Figure 6(b) compares the obtained RL spectrum of Gd^{3+}-doped cane to its PL counterpart under UV excitation. The similarity of RL and PL spectra demonstrates that the RL process involves the same energy levels

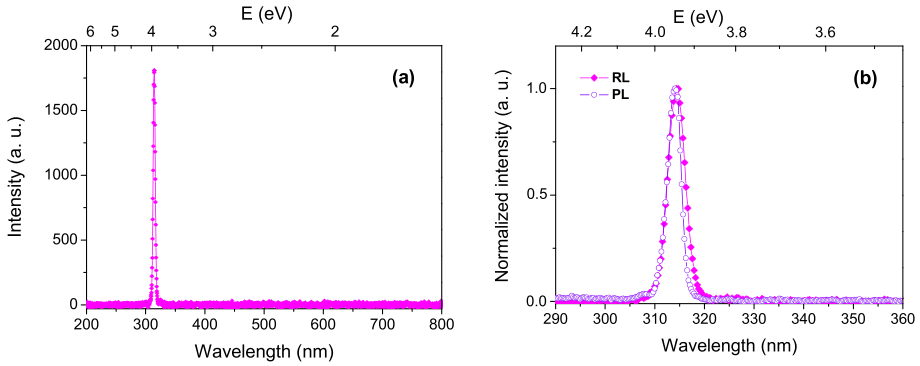

Fig. 6. (a) RL spectrum of Gd^{3+}-doped silica cane in the UV-visible range under 2.1 Gy(SiO_2)/s. (b) Normalized RL (under 2.1 Gy(SiO_2)/s) and PL (under laser excitation at 275 nm) spectra of Gd^{3+}-doped silica cane.

OSA CONTINUUM

as the PL phenomenon: in both cases, the final transition occurs from the $^6P_{7/2}$ level to the $^8S_{7/2}$ ground state of trivalent Gd^{3+} ions. The slight difference between PL and RL bands could be related to the different excitation-emission mechanisms in the PL and RL processes. Regarding the PL case, the gadolinium ions are immediately excited by incident photon energy. Whereas, in the RL, X-rays initially generate electron-hole pairs, which then relax through defect traps before the final radiative recombination on the excited centers.

3. Conclusion

In summary, Gd^{3+}-doped silica glass, with a low doping concentration (0.1 wt%), was prepared using the sol-gel technique. After drawing, the obtained cane sample showed the characteristics UV absorption and luminescence bands associated with Gd^{3+} ions in a silica host. The optical activity of this material in the UV domain was exploited for X-ray radiation dosimetry. We have demonstrated that the RL signal shows a linear response to the dose rate over five decades ranging from 125 µGy/s up to 12.25 Gy/s. Thanks to the obtained results, this material exhibits an interesting potential for remote ionizing radiation dosimetry applications. This Gd^{3+}-activated glass could be suitable for a variety of applications such as a scintillator for other ionizing radiations, energetic particle beams or UV-light sources.

Funding

Agence Nationale de la Recherche (ANR) (ANR-11-EQPX-0017, ANR-11-LABX-0007); Ministère de l'Education Nationale, de l'Enseignement Superieur et de la Recherche (MESR) (CPER Photonics for Society P4S); Région Hauts-de-France (CPER Photonics for Society P4S); European Regional Development Fund (ERDF) (CPER Photonics for Society P4S).

Acknowledgments

We would like to thank K. Delplace for technical assistance. This work has been supported by IRCICA institute, CERLA and FiberTech Lille platforms of University of Lille.

References

1. H. Szmacinski and Q. Chang, "Micro- and Sub-nanosecond Lifetime Measurements Using a UV Light-Emitting Diode," Appl. Spectrosc. **54**(1), 106–109 (2000).
2. T. F. Anderson, T. P. Waldinger, and J. J. Voorhees, "UV-B phototherapy. An overview," Arch. Dermatol. **120**(11), 1502–1507 (1984).
3. T. Koutchma, "UV light for processing foods," Ozone: Sci. Eng. **30**(1), 93–98 (2008).
4. B. Wu and A. Kumar, "Extreme ultraviolet lithography: A review," J. Vac. Sci. Technol. B **25**(6), 1743–1761 (2007).
5. N. Chiodini, A. Vedda, and I. Veronese, "Rare Earth Doped Silica Optical Fibre Sensors for Dosimetry in Medical and Technical Applications," Adv. Opt. **2014**, 1–9 (2014).
6. I. Veronese, N. Chiodini, S. Cialdi, E. d'Ippolito, M. Fasoli, S. Gallo, S. La Torre, E. Mones, A. Vedda, and G. Loi, "Real-time dosimetry with Yb-doped silica optical fibres," Phys. Med. Biol. **62**(10), 4218–4236 (2017).
7. S. Girard, A. Morana, A. Ladaci, T. Robin, L. Mescia, J.-J. Bonnefois, M. Boutillier, J. Mekki, A. Paveau, B. Cadier, E. Marin, Y. Ouerdane, and A. Boukenter, "Recent advances in radiation-hardened fiber-based technologies for space applications," J. Opt. **20**(9), 093001 (2018).
8. P. Ferdinand, S. Magne, and G. Laffont, "Optical fiber sensors to improve the safety of nuclear power plants," Proc. SPIE **8924**, 89242G (2013).
9. P. Ferdinand, S. Magne, O. Roy, V. Dewynter Marty, S. Rougeault, and M. Bugaud, "Optical Fiber Sensors for the Nuclear Environment," In: S. Martellucci, A. N. Chester, and A. G. Mignani, eds. *Optical Sensors and Microsystems* (Springer, 2002).
10. C. Tang, S. Liu, L. Liu, and D. P. Chen, "Luminescence properties of Gd^{3+}-doped borosilicate scintillating glass," J. Lumin. **160**, 317–320 (2015).
11. E. V. Mal'chukova, A. I. Nepomnyashchikh, B. Boizot, T. S. Shamirzaev, and G. Petite, "Luminescence of aluminoborosilicate glasses doped with Gd^{3+} ions," Phys. Solid State **52**(9), 1919–1924 (2010).
12. P. Xu, Z. Fu, S. Fan, H. Lin, C. Li, G. Yao, Q. Chen, Y. Zhou, and F. Zeng, "Study on the sensitization of Gd^{3+} on Ce^{3+}/Tb^{3+} co-doped GBS scintillating glass," J. Non-Cryst. Solids **481**, 441–446 (2018).

OSA CONTINUUM

13. X. Sun, S. Huang, M. Gu, Q. Gao, X. Gong, and Z. Ye, "Enhanced Tb^{3+} luminescence by non-radiative energy transfer from Gd^{3+} in silicate glass," Phys. B **405**(2), 569–572 (2010).
14. Y. Kondo, K. Tanaka, R. Ota, T. Fujii, and Y. Ishikawa, "Time-resolved study of luminescence in soda-lime silicate glasses co-doped with Gd^{3+} and Eu^{3+}," Opt. Mater. **27**(8), 1438–1444 (2005).
15. D. He, C. Yu, J. Cheng, S. Li, and L. Hu, "Energy transfer between Gd^{3+} and Tb^{3+} in phosphate glass," J. Rare Earths **29**(1), 48–51 (2011).
16. P. Szajerski, M. Jakubowska, A. Gasiorowski, and E. Mandowska, "Dosimetric properties of europium, gadolinium and cerium borosilicate glasses in application of electron beam dose measurements," J. Lumin. **182**, 300–311 (2017).
17. S. Girard, B. Tortech, E. Régnier, M. V. Uffelen, A. Gusarov, Y. Ouerdane, J. Baggio, P. Paillet, V. FerletCavrois, A. Boukenter, J.-P. Meunier, F. Berghmans, J. R. Schwank, M. R. Shaneyflet, J. A. Felix, E. Blackmore, and H. Thienpont, "Proton- and Gamma-Induced Effects on Erbium-Doped Optical Fibers," IEEE Trans. Nucl. Sci. **54**(6), 2426–2434 (2007).
18. N. P. Bansal and R. H. Doremus, *Handbook of Glass Properties* (Academic Press, 1986).
19. B. Brichard, P. Borgermans, A. F. Fernandez, K. Lammens, and M. Decreton, "Radiation Effect in Silica Optical Fiber Exposed to Intense Mixed Neutron-Gamma Radiation Field," IEEE Trans. Nucl. Sci. **48**(6), 2069–2073 (2001).
20. O. M. Efimov, K. Gabel, S. V. Garnov, L. B. Glebov, S. Grantham, M. Richardson, and M. J. Soileau, "Color-center generation in silicate glasses exposed to infrared femtosecond pulses," J. Opt. Soc. Am. B **15**(1), 193–199 (1998).
21. B. H. Babu, N. Ollier, M. L. Pichel, H. El Hamzaoui, B. Poumellec, L. Bigot, I. Savelii, M. Bouazaoui, A. Ibarra, and M. Lancry, "Radiation hardening in sol-gel derived Er^{3+}-doped silica glasses," J. Appl. Phys. **118**(12), 123107 (2015).
22. F. Cova, F. Moretti, M. Fasoli, N. Chiodini, K. Pauwels, E. Auffray, M. T. Lucchini, S. Baccaro, A. Cemmi, H. Bártová, and A. Vedda, "Radiation hardness of Ce-doped sol-gel silica fibers for high energy physics applications," Opt. Lett. **43**(4), 903–906 (2018).
23. D. Di Martino, N. Chiodini, M. Fasoli, F. Moretti, A. Vedda, A. Baraldi, E. Buffagni, R. Capelletti, M. Mazzera, M. Nikl, G. Angella, and C. B. Azzoni, "Gd-incorporation and luminescence properties in sol–gel silica glasses," J. Non-Cryst. Solids **354**(32), 3817–3823 (2008).
24. Y. Wang, J. He, P. Barua, N. Chiodini, S. Steigenberger, M. I. M. Abdul Khudus, J. K. Sahu, M. Beresna, and G. Brambilla, "Ultraviolet photoluminescence in Gd-doped silica and phosphosilicate fibers," APL Photon. **2**(4), 046101 (2017).
25. H. El Hamzaoui, L. Courthéoux, V. Nguyen, E. Berrier, A. Favre, L. Bigot, M. Bouazaoui, and B. Capoen, "From porous silica xerogels to bulk optical glasses: The control of densification," Mater. Chem. Phys. **121**(1-2), 83–88 (2010).
26. H. El Hamzaoui, M. Bouazaoui, and B. Capoen, "Raman investigation of germanium- and phosphorus-doping effects on the structure of sol-gel silica-based optical fiber preforms," J. Mol. Struct. **1099**, 77–82 (2015).
27. E. Duval, A. Boukenter, and T. Achibat, "Vibrational dynamics and the structure of glasses," J. Phys. Condens. Matter **2**(51), 10227–10234 (1990).
28. F. Moretti, N. Chiodini, M. Fasoli, L. Griguta, and A. Vedda, "Optical absorption and emission properties of Gd^{3+} in silica host," J. Lumin. **126**(2), 759–763 (2007).
29. J. He, Y. Wang, S. Steigenberger, A. Macpherson, N. Chiodini, and G. Brambilla, "Intense ultraviolet photoluminescence at 314 nm in Gd^{3+}-doped silica," in *Conference on Lasers and Electro-Optics, OSA Technical Digest (2016)* (Optical Society of America, 2016), paper JTh2A.86.
30. M. Cardona, R. V. Chamberlin, and W. Marx, "The history of the stretched exponential function," Ann. Phys. (Leipzig) **16**(12), 842–845 (2007).
31. M. Berberan-Santos, E. N. Bodunov, and B. Valeur, "History of the Kohlrausch (stretched exponential) function: Pioneering work in luminescence," Ann. Phys. (Berlin) **17**(7), 460–461 (2008).
32. D. C. Johnston, "Stretched exponential relaxation arising from a continuous sum of exponential decays," Phys. Rev. B **74**(18), 184430 (2006).
33. J. H. Hubbell and S. M. Seltzer, "X-Ray Mass Attenuation Coefficients," Radiation Physics Division, PML, NIST, 1996.
34. N. Al Helou, H. El Hamzaoui, B. Capoen, G. Bouwmans, A. Cassez, Y. Ouerdane, A. Boukenter, S. Girard, G. Chadeyron, R. Mahiou, and M. Bouazaoui, "Radioluminescence and Optically Stimulated Luminescence Responses of a Cerium-Doped Sol-Gel Silica Glass Under X-Ray Beam Irradiation," IEEE Trans. Nucl. Sci. **65**(8), 1591–1597 (2018).
35. A. K. M. Mizanur Rahman, M. Begum, M. Begum, H. T. Zubair, H. A. Abdul-Rashid, Z. Yusoff, and D. A. Bradley, "Radioluminescence of Ge-doped silica optical fibre and Al_2O_3:C dosimeters," Sens. Actuators A **270**, 72–78 (2018).
36. A. J. Miller, R. G. Leisure, and Wm. R. Austin, "X-ray induced luminescence of high-purity, amorphous silicon dioxide," J. Appl. Phys. **86**(4), 2042–2050 (1999).